A CUBESAT DERIVED DESIGN FOR A UNIQUE ACADEMIC RESEARCH MISSION IN EARTHQUAKE SIGNATURE DETECTION

Matthew Long, Allen Lorenz, Greg Rodgers, Eric Tapio, Glenn Tran,
Keoki Jackson and Robert Twiggs

Aeronautics & Astronautics
Stanford University

Thomas Bleier
Stellar Solutions

Abstract. CubeSats are playing a vital role in the development of new micro-sized components for small satellites, and because of their promising potential CubeSats have been widely embraced by universities for conducting space research projects. Now, CubeSats are being proven to be an effective small satellite design, which have the ability to be easily modified to accommodate larger academic and even commercial scientific missions. QuakeSat, a small satellite currently being developed by the Space Systems Development Laboratory (SSDL) at Stanford University will be launched to study earthquake precursor phenomena from space. QuakeSat's primary scientific mission is to detect, record, and downlink Extremely Low Frequency (ELF) magnetic signal data, which may lead to groundbreaking techniques to predict earthquake activity. Set to launch in 2003, and bound for a 650 km sun-synchronous orbit, QuakeSat is a prime example of CubeSat technology, which utilizes commercially-off-the-shelf (COTS) components originally used in non-space applications and using them for scientific experiments and payloads, providing a low cost alternative to launch space missions, and support small-satellite infrastructure in the near future.

1.0 Introduction

It is known that when earthquakes (Richter scale magnitude of 6 or larger) develop that the layers of bedrock in the Earth's crust begin to fracture as stress builds along the fault lines. One theory states that fracturing of the bedrock creates the ELF magnetic waves. These signatures radiate from the earthquake hypocenter region (several tens of square kilometers), through the earth (5-80 km), through the atmosphere to the Ionosphere (100-200km), and are propagated up the Earth's magnetic field lines to the satellite altitude (600-900 km.). As a result, there is considerable interest in determining whether the ground-based ELF magnetic signatures associated with earthquakes (Ref. 1) can be detected at the considerable altitude of a satellite, in this case in a circular, low earth orbit, with a 600-900 km altitude.

A Russian satellite, Cosmos 1809 (Ref. 2), detected 140 Hz and 450 Hz signals just after a M6+ earthquake in Spitak, Armenia in 1989 every time the satellite passed within ± 6deg of Lat. and Long. of the earthquake (offset by approx. 6 deg in Lat.). A French satellite, Aureol 3, (Ref. 3) also detected similar readings in a worldwide survey of ELF frequencies over active earthquake regions.

Therefore, the QuakeSat mission objectives are to detect, record, and downlink the ELF

magnetic data to verify the results from these prior experiments. In addition, it is hoped that investigating the ELF data can ultimately lead to the prediction of earthquakes of magnitude 6.0 or higher.

QuakeSat will help determine if the CubeSat paradigm is a cost-effective platform for conducting significant scientific research experiments in space. It is hoped to demonstrate the feasibility of utilizing Commercial-Off-The-Shelf (COTS) parts to construct a reliable, short-mission micro-satellite.

QuakeSat, shown in Fig. 1, will be launched in 2003 and is designed for a nominal one yearlong mission life. QuakeSat will be deployed into a sun-synchronous, Low-Earth Orbit (LEO) at an altitude of 650 km

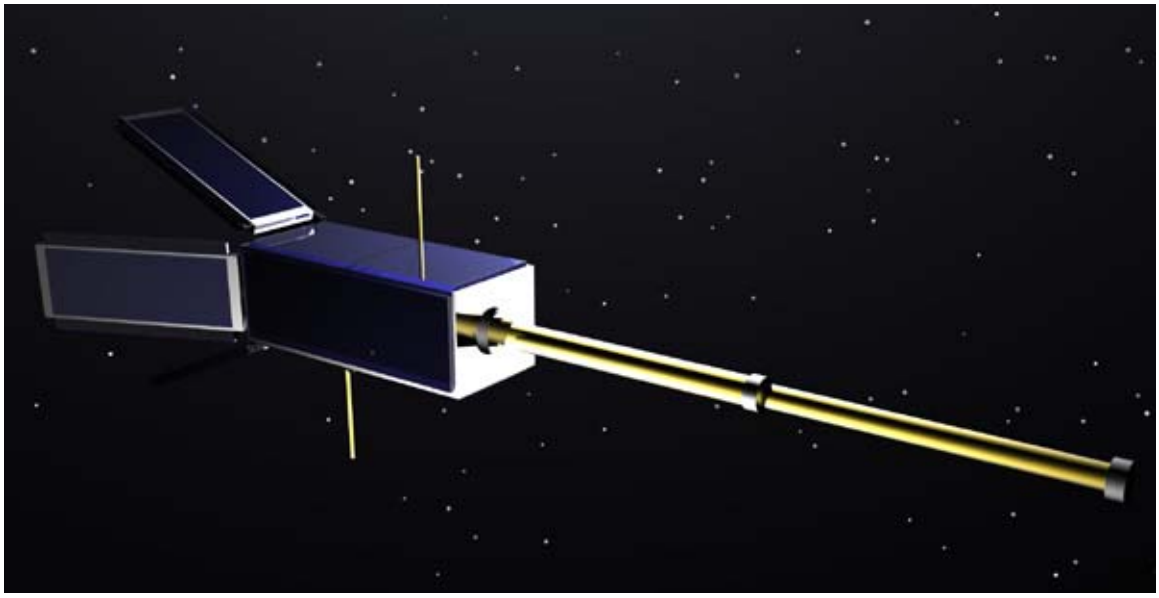

Figure 1: QuakeSat in Deployed Configuration

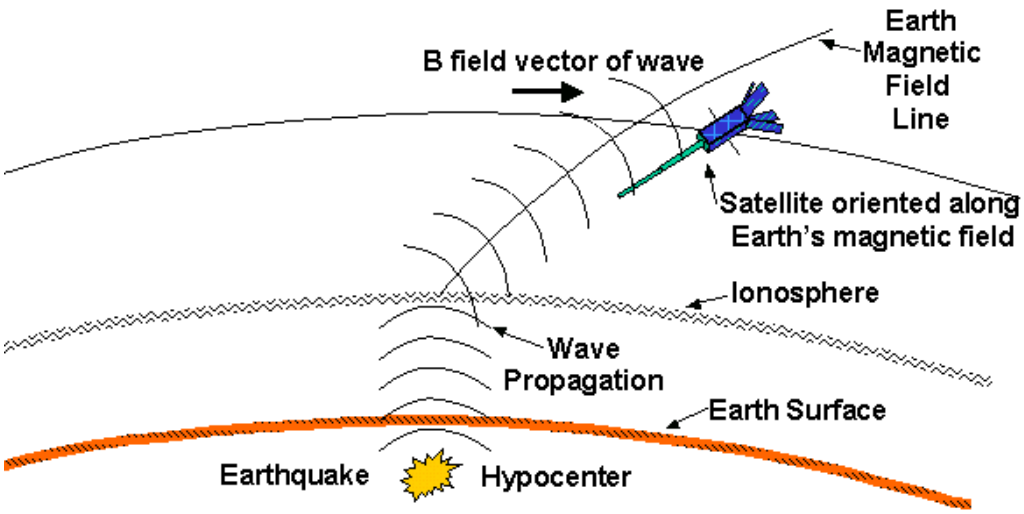

Figure 2: QuakeSat Misison Concept

Figure 2 illustrates the QuakeSat mission concept. The ELF waves refract in the Ionosphere and propagate into space along the Earth's magnetic field lines. QuakeSat will use permanent magnets for passive attitude control to orient the QuakeSat close to the magnetic field line, as shown in Fig. 2. A 0.701 m deployable payload boom contains the commandable ELF magnetometer, which collects raw ELF data. The deployable boom is necessary to shield the ELF sensor from any internal magnetic disturbances generated by the QuakeSat electronics.

2.0 Payload Description

The strategy used to detect the small magnetic field measurements (0.5 to 1000 Hz) relies on the use of a very sensitive AC magnetometer. The ELF sensor is a single axis, search coil (induction) magnetometer with multiple frequency bands. It is similar to a network of ground-based magnetometers that are being built and deployed along the California fault zones. The magnetometer is 0.305 m long and 0.019 m in diameter. Figure 3 shows the placement of the magnetometer in the boom.

There is no on-board processing of the mission data, other than multiple, analog low pass, high pass, and pass band filters. Figure 4 contains a block diagram of the payload and the QuakeSat architecture. All electronics are contained on a single printed circuit board. The payload was designed for simplicity, but was modified to select specific frequency bands and only power those bands to keep the overall power usage to a minimum.

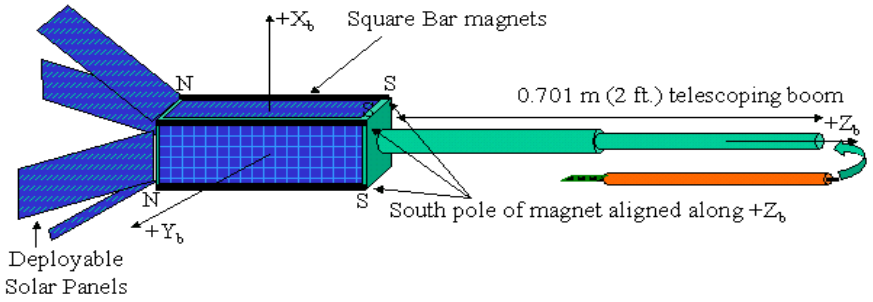

Figure 3: Overview of ELF sensor on Deployable Boom

QuakeSat Architecture Block Diagram

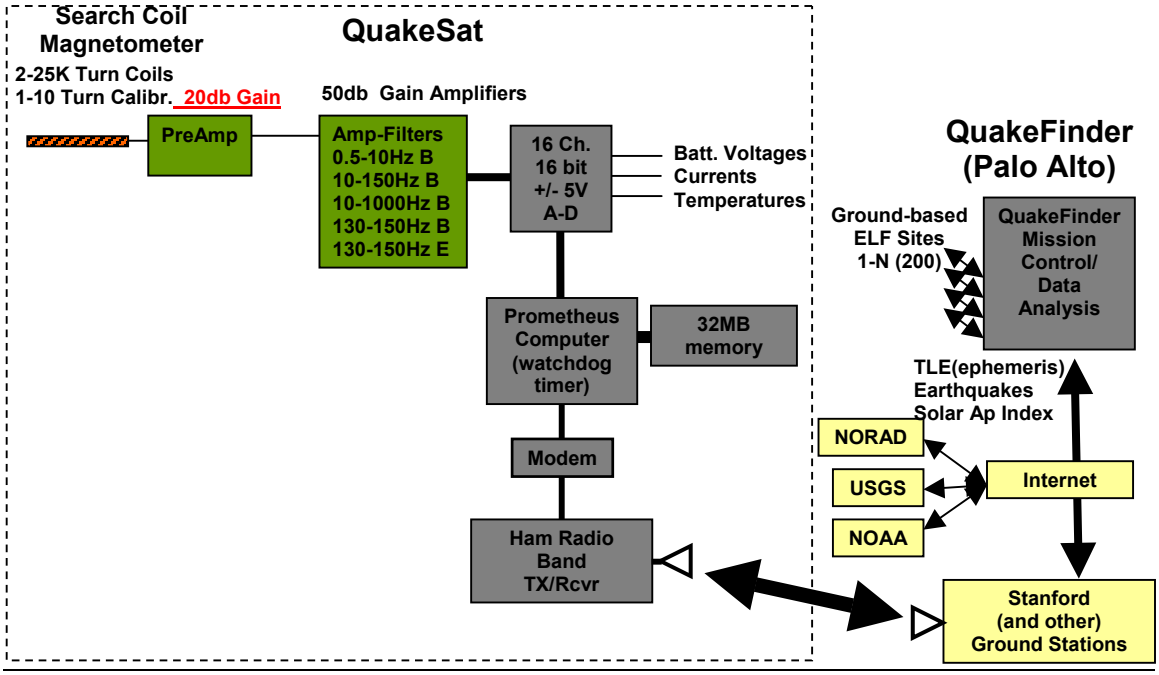

Figure 4: QuakeSat Architecture Block Diagram

The QuakeSat frequency bands for the ELF payload are:

Band 1: 0.5 to 10 Hz narrow band magnetic; Band 2: 10 Hz to 150 Hz wide band magnetic; Band 3: 10 Hz to 1000 Hz wide band magnetic; Band 4: 130-150 Hz narrow band magnetic; Band 5: 130-150 Hz narrow band electric field. All the bands are sampled at 2-3x their highest frequency, except the 130-150 Hz band, which is sampled at 1/sec. The preamps and 130-150 Hz magnetic and electric field band filters are powered whenever data is taken so that the index of refraction and Poynting calculated to

determine whether or not the ELF wave is propagating upward or downward.

During a data gathering event, one of the other wideband or narrow band filters is also commanded on, and the sample rate is adjusted accordingly. There is also a commandable 10 Hz calibration signal that causes a known current to be injected in a co-axial 10-turn calibration coil on the magnetometer. This results in a known magnetic field over the magnetometer coil and verifies that the preamplifier and amplifiers are working properly. This calibration signal is commanded on for 10 sec. prior to every data acquisition event.

3.0 Structure

The QuakeSat nano-satellite is a variation of the CubeSat design, developed jointly by Stanford University and Cal Poly San Luis Obispo. QuakeSat is an elongated CubeSat design that has the length equal to three CubeSat's. It measures slightly more than 10 x 10 x 30 cm and weighs 3 kg. Stacking three CubeSats together allows magnetometer payload, which has an overall length of nearly 30 cm, to fit inside the structure after being attached to the end of the deployable boom (shown in Fig. 3).

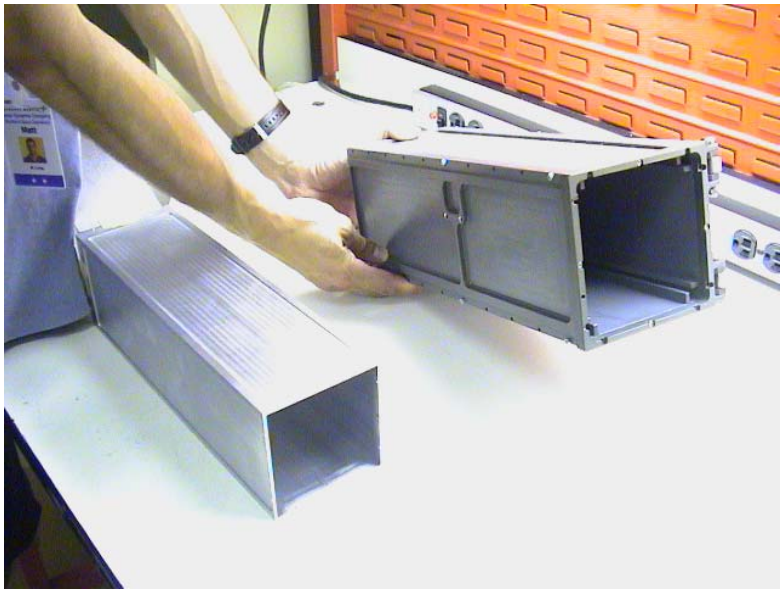

Figure 5: QuakeSat Outer Structure (lower left) and P-Pod Launcher (upper right)

The outer structure is 6061 Aluminum and fits inside the P-Pod launch tube, shown in Fig. 5. The P-Pod launch tube is what will be bolted to the launch vehicle upper state and contains a spring-loaded pusher foot that will eject QuakeSat via ground command. The outer structure along with the four body mounted solar arrays have sufficient clearance inside the P-Pod. It can be seen in Fig. 3 that the four deployable arrays are folded on top of the body-mounted arrays and will deploy automatically using spring loaded hinges once the QuakeSat is clear of the P-Pod.

The 0.701 spring-loaded telescoping boom is also made of aluminum, and is completely contained within the QuakeSat structure prior to deployment. The details of the boom structure are listed below:

Boom Specifications:
Total boom length: 0.701 m
–Seg 1: Dia: 38 mm, Length: 0.35 m
–Seg 2: Dia: 32 mm, Length: 0.35 m
–Seg 3: Dia: 25 mm, Length: 0.36 m
Boom material: Aluminum
Boom mass: 0.4536 kg
Total mass (boom + sensor): 0.8221 kg

Upon ejection from the P-Pod, the boom will automatically deploy and "lock" once fully extended.

A preliminary mass properties analysis was performed and it was determined that the moments of inertia for QuakeSat are the following:

Table 3.1: QuakeSat Mass Properties

	C.M. (m)	I_{xx} (kg-m^2)	I_{yy} (kg-m^2)	I_{zz} (kg-m^2)	I_{xy} (kg-m^2)	I_{xz} (kg-m^2)	I_{yz} (kg-m^2)
Stowed	0, 0, 0	0.025	0.025	0.025	0	0	0
Deployed	0, 0, 0.063	0.313	0.313	0.017	0	0	0

Because the spacecraft is symmetric when the solar arrays and boom are fully deployed, the products of inertia are zero and the center of mass only shifts along the boom axis.

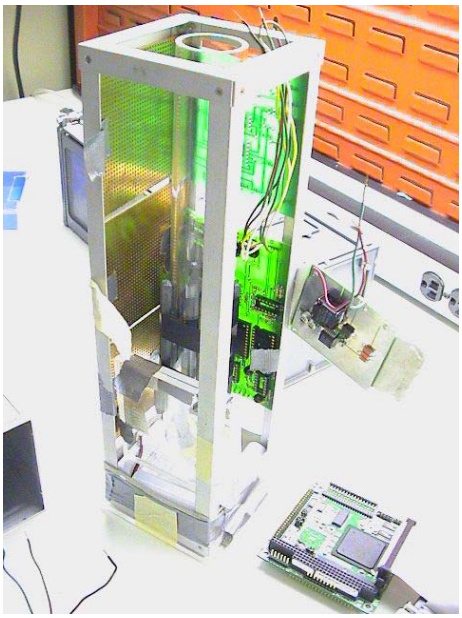

Figure 6. QuakeSat Inner Structure

QuakeSat also contains an inner rack structure that slides inside the outer structure in Fig.5. Figure 6 depicts the inner structure with the boom in the center of the rack. The flight hardware and circuit boards are fastened to the inner rack and arranged so the components fit around the boom. Because the QuakeSat outer structure is one-piece, the inner structure provides a convenient way to work on the

electronics by simply pulling out the inner rack.

4.0 Command and Data Handling

QuakeSat's Command and Data handling (C&DH) is designed to operate with stored, timed commands to synchronize payload data gathering with historically active (M6+) earthquake areas. To sample the data, the world is mapped into grid of 5° squares of latitude and longitude. This 5° resolution was derived to allow the sensor to be turned on and calibrated prior to passing over area of high earthquake activity. Also by using a 5° grid, the selected earthquake areas results in a 15% duty cycle for the payload, resulting in dramatically reduced power requirements.

The position of QuakeSat on the world map is determined through NORAD Two Line Element Sets (TLEs) and a ground-based propagator. TLE data sets are estimated to give a error in position of approximately 10 km or less. The world map and the TLE propagation algorithms will not be stored in the QuakeSat C&DH. The determination of QuakeSat's orbital position will be calculated on the ground and a table of payload turn-on and turn-off times that correspond to QuakeSat's movement through each 5 degree box on the map will be uploaded and allow the C&DH to collect ELF data throughout QuakeSat's orbit.

The ELF data will then be downlinked through one or more ground stations. However, QuakeSat will be able to store at least one day's commands and data in case a ground station is unavailable or QuakeSat is unable to transmit the data for any reason (e.g. low power reserves). QuakeSat will also accommodate changes in sample rates of the payload, and allow for direct on/off commanding of the payload as directed by the ground.

Figure 7: Prometheus PC/104 CPU module

A capable CPU was selected to give was to give QuakeSat enough capability to satisfy the C&DH requirements. The Prometheus central processing unit (CPU) module with Ethernet and data acquisition all on a single board from Diamond Systems, shown in Fig. 7, is a PC-104 form factor processor, with 32 megabytes (MB) of memory, and a 192 MB flash disk.

The Prometheus processor was selected based on its wide operational temperature range (–40 to +85 °C), and 16 channels of 16-bit analog input. The Prometheus also has hardware and software watchdog timers, and boots to normal operations within 30 seconds. The Linux operating system was selected to control the Prometheus CPU. Linux is ideal for QuakeSat because a device driver already exists for communications with the Bay Pac modem, AX.25 libraries and utilities, along with several other system utilities used in the amateur satellite/ham radio world.

QuakeSat will also contain between 48 housekeeping sensors. These sensors will measure the currents on the 12 solar arrays, the current drawn by the payload, computer, and transmitter, the voltages for the batteries and solar panels, and the regulated ±5 volt bus. Temperatures for the batteries, transmitter, computer, payload and QuakeSat structure will also be monitored. The sample rate for all housekeeping sensors will be configurable between 1 Hz and 0.1 Hz. Telemetry from the solar panel currents will be used to estimate the QuakeSat's attitude from the local sun vector.

5.0 Communications

The major components of the QuakeSat communications subsystem are a Tekk T-Net Mini 9600 Baud, half duplex crystal controlled radio and a Bay Pac 9600 modem. The communications hardware is shown in Fig. 8 connected to the Prometheus using a serial connection. The Tekk radio is one of the smallest 9600 Baud data packet radios found off the shelf with 2 Watts of RF output. The communications system uses the UHF frequency (436.675 MHz) for both transmit and receive. QuakeSat has 37.1 dB for link margin on uplink and 34.9 dB margin on downlink. The AX.25 protocol, standard in the ham radio community, is being used for the communication protocol.

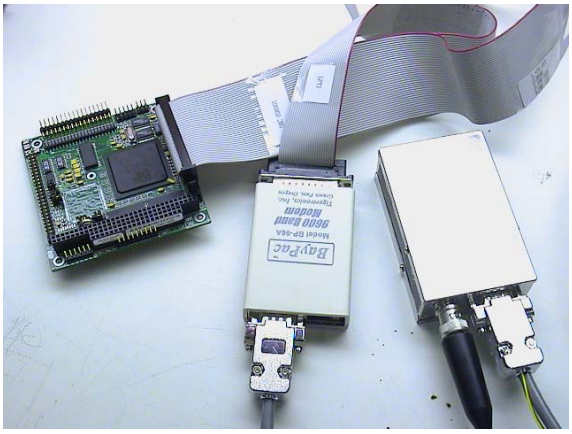

Figure 8: Bay Pac Modem and Tekk Radio

One of the major challenges encountered by the QuakeSat team was the multiple data sampling rates required by the payload. Payload data will account for over 97% of all data coming down from the spacecraft. QuakeSat will download up to 3.0 MB / per day. Data loading calculations assumed up to 3000 samples/sec, 50% overhead, 2-to-1 data

compression (via Bzip2), and 2 ground stations. The overall data loading required a 9600-baud communication system to be able to downlink all the ELF data during each pass over the ground station.

QuakeSat has four antennas that are a quarter wavelength long (70 mm) and 6.3 mm wide to transmit and receive on the UHF band. All four antennas are made of spring steel tape measure material. Each antenna is mounted on the four corners of the spacecraft body at 45° as shown in Fig. 9. The dotted lines depict the E-field ELF antennas at the end of the solar arrays.

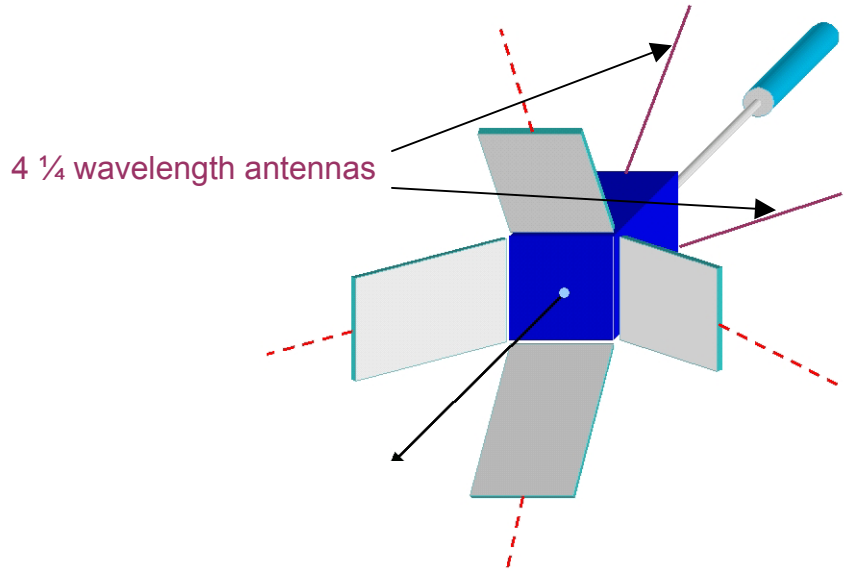

Figure 9: Antenna Placement

The antennas are stowed between the deployable and body mounted arrays and will automatically deploy once the solar arrays are deployed.

6.0 Electrical Power System

The QuakeSat Electrical Power System (EPS) includes three subsystems: a power source, power storage, and a power regulator. Figure 10 is a schematic of the EPS system.

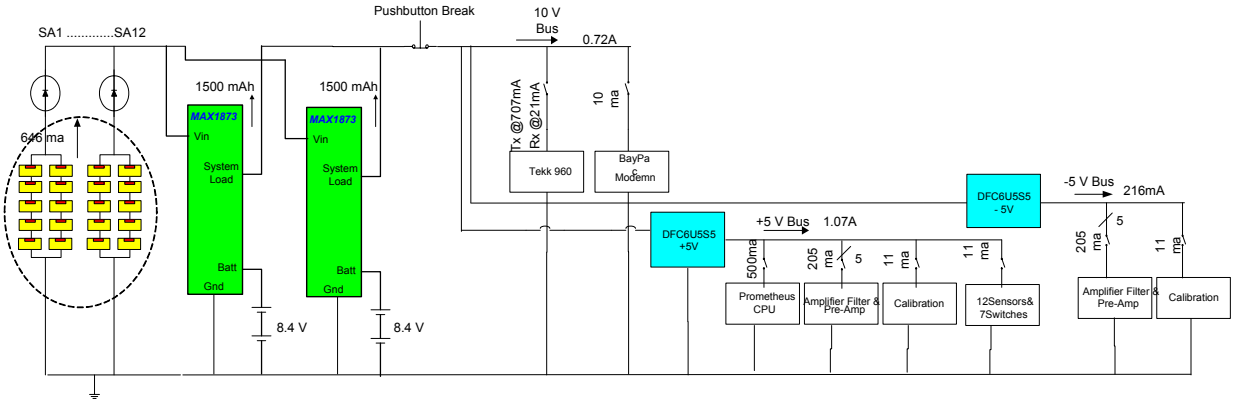

Figure 10: QuakeSat's Electrical Power System

The power source consists of twelve solar arrays: four body mounted panels and four are double sided deployable wings (see Fig. 3). The double-sided arrays are canted at 150° relative to the QuakeSat body. The 150° cant angle was found through a power/attitude simulation to yield the maximum amount of power due to the high sun angle experienced in the sun synchronous orbit. The simulation showed that the solar arrays at a 150° cant angle would generate between 7.90 W to 19.05 W depending on the time of year. These power levels will adequately cover the system loads, which are expected to be between 2.8 W (min) and 12.6 W (peak). Each solar array is 330 x 86 mm and the ten multi-junction GaAs solar cells on each array have an efficiency of 22.9%. The cells on each array are made up of two parallel strings, five cells in series per string, and produces 6.46 W as shown in Fig. 11.

The power storage subsystem in Fig. 12 includes two MAX1873 Li+ charge controllers (Ref. 4) and four Li+ Ion batteries, 2-series Li+ batteries per branch and 2 parallel-branches. The MAX1873 is capable of supplying power to the system load during daylight, while charging 3 Li+ cells in series. A chip in the MAX1873 kit was replaced so that 2 instead of 3 Li+ batteries could be charged. Each charge controller limits the total source current and the maximum charging current to 3 A, to charge 2-series Li+ cells up to 4.2 V each, and to power the satellite function. The power regulator (Ref. 5) consists of two DFC6U5S5 voltage regulators that convert the unregulated solar panel bus voltages of 9.6 V and 7.5 V during daylight and eclipse respectively, to regulated +5 V and –5 V payload buses. The +5 V bus supplies the power to the CPU and the payload, and the –5 V bus supplies the payload only. The system bus also supplies the power directly to the Tekk 960 radio.

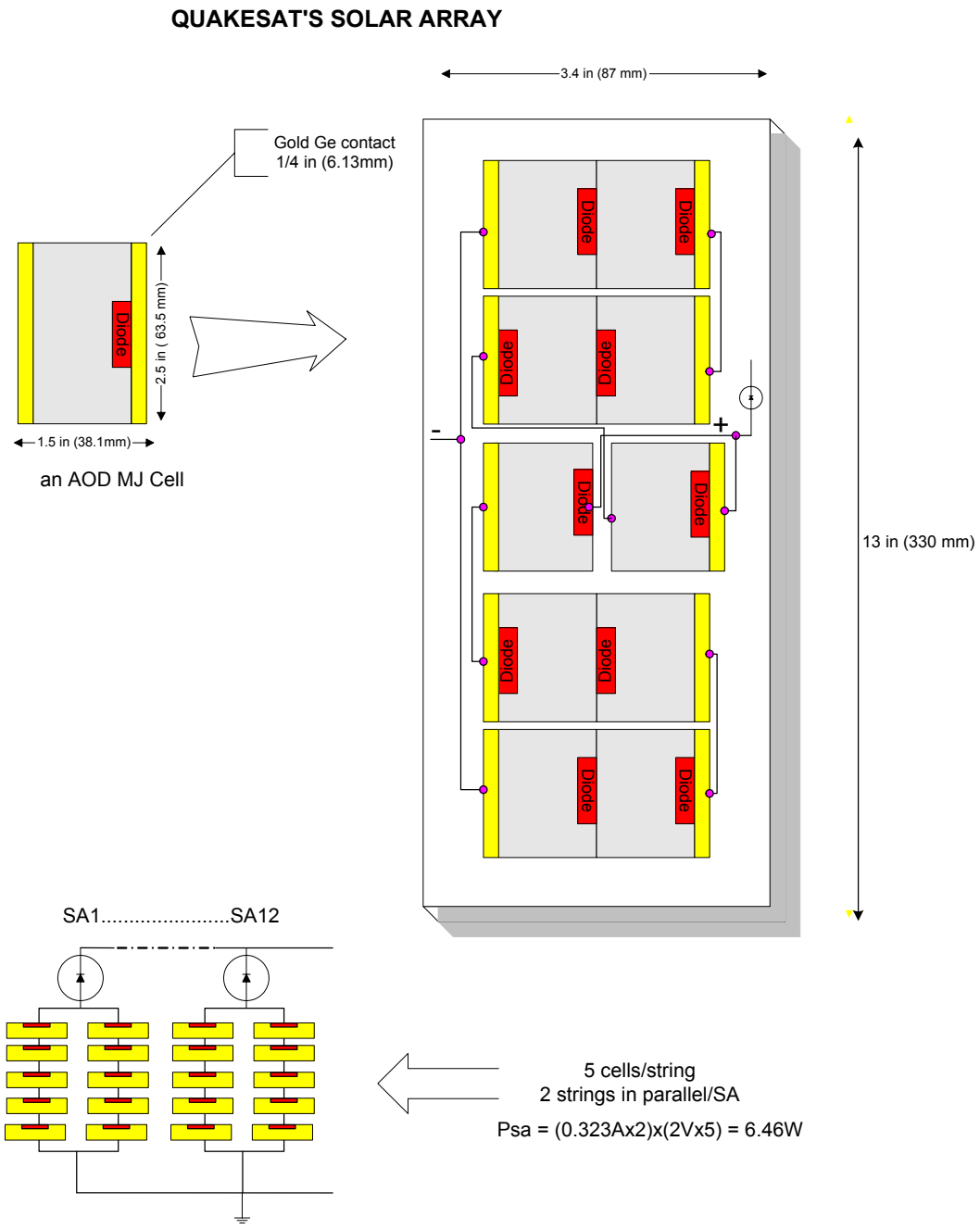

Figure 11: QuakeSat Solar Array Schematic

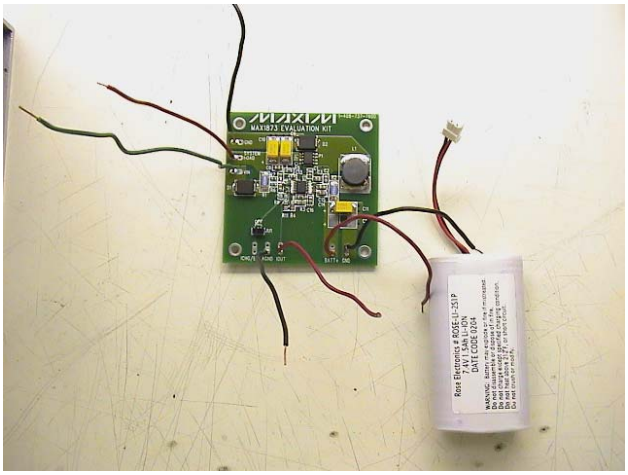

Figure 12: Max1873 Li+ Charger Controller and 2-Series Cells

7.0 Thermal Analysis

QuakeSat uses passive thermal control. The thermal analysis, derived using the analysis in Sec. 11.5 of Ref. 6 shows that the temperature excursion is expected to be between 27°C and –38°C. The results of the analysis found in Figs. 13 and 14 indicate that temperatures are within the upper temperature limit but occasionally fall below the lower temperature limit of the Tekk 960 and the Li+ discharge range. Updated payload and transmitter heat dissipation rates may help the lower temperature estimates.

Figure 15 shows the predicted thermal profile of the Quakesat. It depicts two thermal cycles that mimic the orbit period of the Quakesat. The 65 minutes at the hot level and 33 minutes of cold are equivalent to 65 minutes daylight and 33 minutes eclipse respectively.

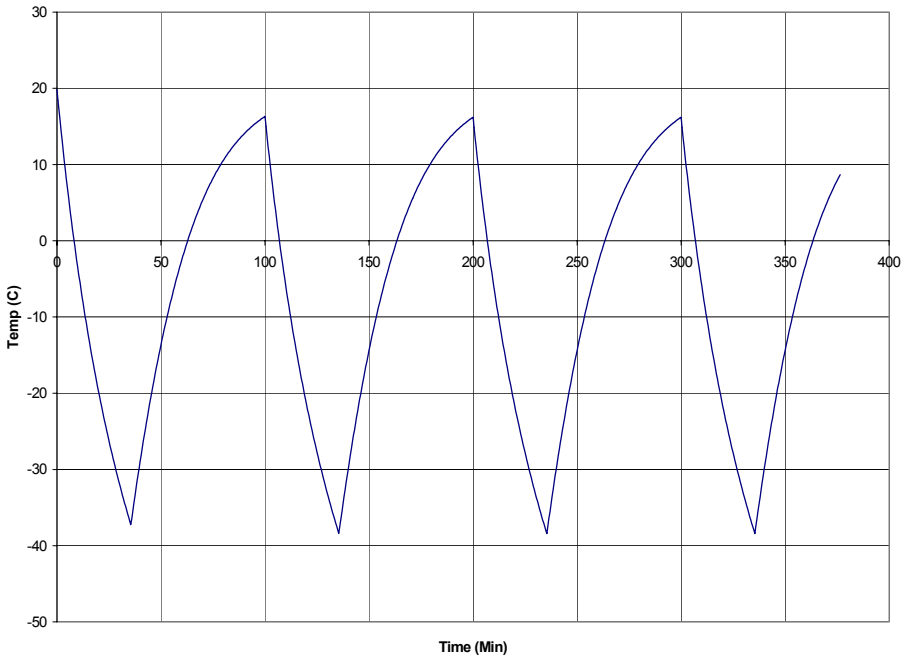

Figure 13: QuakeSat Transient Effects Temperature

Company	Component	Tmin	Tmax
Tekk	Tekk960	-30	60
BayPac	Modem	TBD	TBD
Diamond Systems	CPU	-40	85
Rose Electronics	PL, Power	-40	125
Maxim	Battery Charger	0	45
Maxim	Battery Discharger	-10	60
	QuakeSat	-38	27

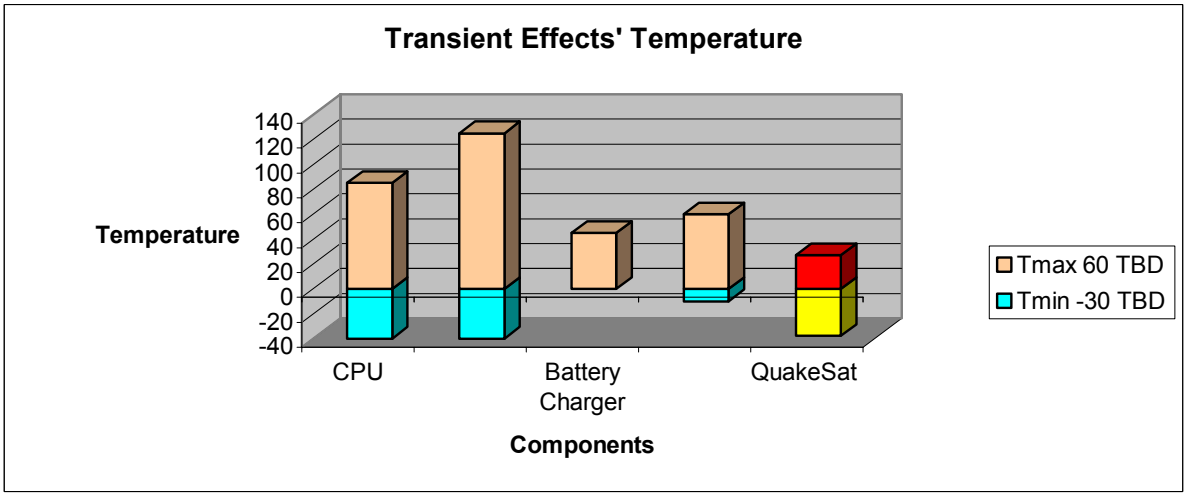

Figure 14: Component Temperature Analysis

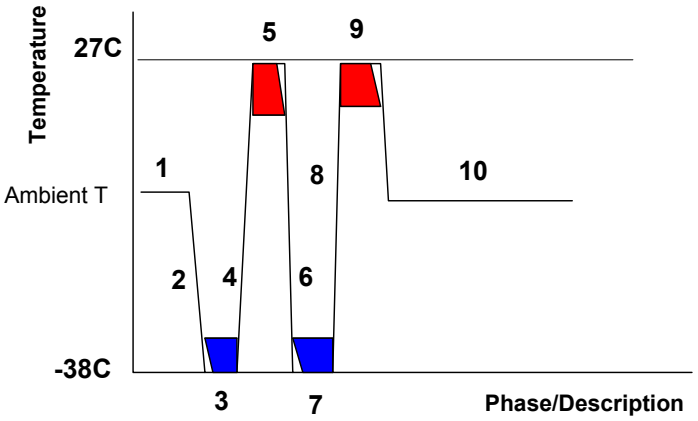

1) Ambient Temperature: Turn on the QuakeSat system for functional check
2) Ambient to Cold 1 in 20 minutes
3) Cold 1: 35 minutes
4) Cold 1 to Hot 1 in 60 minutes
5) Hot 1: 65 minutes
6) Hot 1 to Cold 2 in 35 minutes
7) Cold 2: 35 minutes
8) Cold 2 to Hot 2 in 60 minutes
9) Hot 2: 65 minutes
10) Hot 2 to Ambient in 20 minutes

Figure 15: Predicted Thermal Cycle of QuakeSat

8.0 Attitude Determination and Control

Permanent magnets are used for attitude control to keep the ELF magnetometer aligned close to the Earth's magnetic field. QuakeSat uses four ALNICO 8HE magnets that are 6.35 x 6.35 x 102 mm long. Each magnet weighs 0.224 kg. Permanent magnets have been used for passive control on other amateur spacecraft (Refs. 7 and 8). The ALNICO 8 HE magnets were chosen because of their higher resistance to demagnetization.

The four magnets are attached to the inner boom inside the QuakeSat bus as shown in Fig.16.

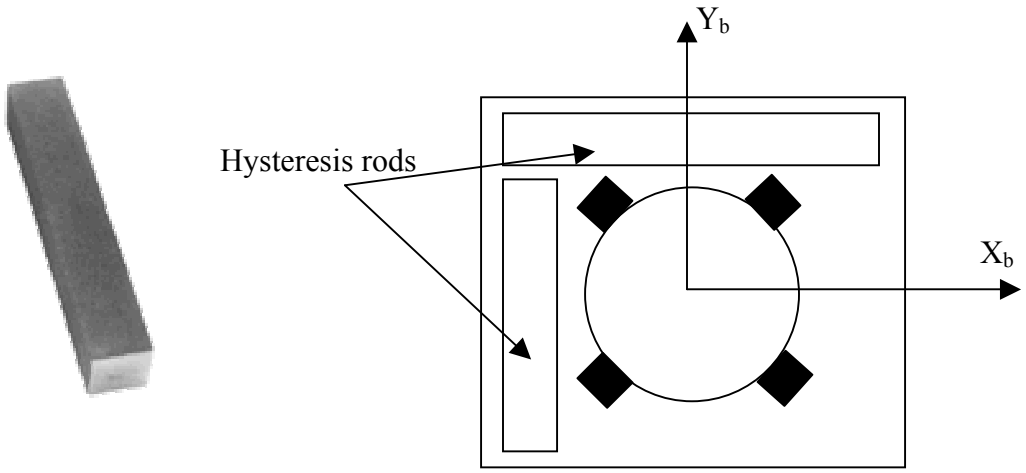

Figure 16: ALNICO 8 HE Magnet and Location in QuakeSat

By aligning the magnets along the boom axis, QuakeSat will fly nearly parallel to the magnetic field lines as QuakeSat rotates twice per orbit about an axis perpendicular to the boom ($+Z_b$) axis. The QuakeSat boom will be nadir pointing over the North Pole and zenith pointing over the South Pole. To help minimize the librations as QuakeSat tumbles over the poles, two hysteresis rods made from Carpenter 49 High permeability alloy (Refs. 9 and 10), will be mounted along the $+X_b$ and $+Y_b$ axes for damping.

The dipole moment produced by the 8HE magnets can be calculated from the following:

$$d_m = \frac{B_r V_m}{\mu_o} \qquad \text{(Eq. 8.1)}$$

where:

μ_0 = magnetic permeability in vacuum 1.257 x 10^{-6} N-A^{2}B$_r$ = magnetic material residual inductance (Tesla)V$_m$ = Volume of bar magnet. The dipole moment analysis yields a value of d_m = 2.933 A-m^2 for the 8 HE magnets. The amount of restoring torque the magnets produce is found by:

$$T_{restore} = d_m B \sin(\theta_m)$$

$$B = \frac{2M}{R^3} \qquad \text{(Eq. 8.2)}$$

where d_m is the value from Eq. 8.1 and,

B = magnetic field model from Ref. 6 (4.95 x 10^{-5} Tesla for a 650 km altitude)

M = magnetic moment of Earth , 7.96 x 10^{15} Tesla-m^3

R = radius from dipole center to s/c (m)

θ_m = angle the dipole moment makes with respect to the Earth's magnetic field.

Using Eq. 8.2 and assuming that $\theta_m = 10°$, the amount of restoring torque for one 8 HE magnet is 2.33 x 10^{-5} N-m, which is the same magnitude as the magnetic field.

Using the equations in Ref. 6 for environmental disturbance torques, it was found that the worst-case disturbance torque magnitudes are:

Aerodynamic torque: ≈1.1 x 10^{-8} N-m
Gravity Gradient: ≈5.1x 10^{-8} N-m
Solar Rad Pressure: ≈2.6 x 10^{-8} N-m

Comparing these values to the restoring torque of the 8 HE magnets, it can be seen that the magnetic control torque can overcome the on-orbit disturbances.

Solar array current measurements will be used to determine the attitude with respect to the sun (Ref. 8). QuakeSat cannot determine attitude with respect the Earth since there is no attitude determination hardware on-board. However, because the current from the solar arrays changes almost instantaneously as a function of the sun angle on the solar panel, the incidence angle for at least two panels can be calculated every time telemetry is sampled. Determining the incidence angle for several panels can allow us to make a crude guess as to where the spacecraft is pointing relative to the sun and earth. As presented in Ref. 8, the equation for the incidence angle is as follows:

$$\theta = 90^\circ - a\cos\left(\frac{I_{now}}{I_{\max}}\right) \qquad \text{(Eq. 8.3)}$$

where θ is the incident angle, I_{now} is the actual current measured, and I_{max} is the maximum current the panel is capable of producing. The discussion in Ref. 8 also indicates that Eq. 8.3 is accurate above 15° of sun angle. The attitude measurement will be used to determine how close the ELF sensor is aligned to the Earth's magnetic field and how much of an ELF signal is measured. When the antenna is horizontal, the output is maximum, and

when vertical, it is zero, referenced to the ELF wave vector.

The ELF sensor also cannot experience a spin rate higher than 1 deg/sec before the introduced noise interferes with the magnetic data. Examining solar array currents over time and measuring the time between the peaks of the currents will determine the spin rate for QuakeSat. Measuring the spin rate will also help to decide if the ELF data is of good quality.

9.0 Ground Station Operations

Once QuakeSat is launched and the magnetometer boom and solar panels are deployed, the satellite is commanded through the QuakeSat ground station. The architecture presented in Fig. 4 shows the how the data will flow between the satellite and the groundstation.

Once on-orbit, the satellite will be given a satellite ID number for tracking purposes, and the TLE will be downloaded from a web site each day. The ephemeris will be propagated forward in time to determine the position/time of the satellite for the next 24-48 hrs. Pre-determined areas of interest will be compared against the satellite track and appropriate payload on-off times will be computed using the world map, the time of the last onboard clock counter initialization, and the present time (accurate to at least 10 ms). The groundstation will determine which frequency band will give the best data (based on flight experience), and then generate a file of channel on-off times. These times will be converted to satellite on-board computer clock times (counts), and the resulting file will be readied for uploading to the QuakeSat C&DH through the Stanford CubeSat groundstation.

When the on-board clock reaches the proper time, individual payload power switches will be toggled as the satellite flies over a desired earthquake area. The calibration subsystem will be commanded on for 10 sec. at the start of every data collection event, followed by the selected filter channel on command for a duration calculated to cover the entire earthquake area. The resulting data file will be compressed and stored in computer memory for the next available ground station pass. Based on a pre-coordinated schedule, QuakeSat will download the data files, with satellite ID, to the ground station computer. Subsequently, it will be automatically transmitted using File Transfer Protocol (FTP) to QuakeFinder headquarters and analyzed in their mission data analysis center as shown in Fig. 3.

In addition to the payload data collection, the ground operator will be able to query real-time data from any individual sensor, or operate any individual switch. This functionality will be required for conducting on orbit checkout of the satellite. Every three days, the operator will also need to synchronize the onboard clock, which is implemented as a hardware counter incrementing in 10 ms steps. The operator can next request a download of any real-time payload sensor, or payload archived data.

10.0 Conclusion

We have shown in this paper that the QuakeSat, a derivative of the CubeSat class of spacecraft, is an effective small satellite design, and may be easily modified to accommodate larger academic and even commercial scientific missions. QuakeSat is to be built and launched for ≈$177,000 (parts and launch costs only). Therefore, QuakeSat should prove that the CubeSat class of satellites can provide a low cost alternative to larger multiple-payload space missions, and

can support smaller single instrument commercial or research missions in the near future.

This paper described an overview of the Extremely Low Frequency (ELF) magnetic signatures detection mission to be flown on QuakeSat. Other instruments have demonstrated the ability to detect earthquake-related ELF magnetic signals on the ground, QuakeSat's mission goal is to verify that the ELF signatures can also be detected from LEO, and in some cases compared directly to the simultaneous ground data from a similar instrument. Periodic analysis reports will be generated based on the ELF data and the occurrence of Magnitude 6+ earthquakes around the world. This analysis will indicate whether ELF signals can be reliably detected by a satellite before and after large earthquakes, and determine what conditions are required (earthquake size, type, depth, of location) for detection?

Acknowledgements

This work was performed in the Stanford Space Systems Development Laboratory with sponsorship from Stellar Solutions and Lockheed Martin.

References

1. A.C. Fraser Smith, et. al., "Low-frequency magnetic field measurements near the epicenter of the Ms 7.1 Loma Prieta earthquake", Geophysical Research Letters, Vol. 17, No. 9, pages 1465-1468, August 1990.
2. O.N. Serebryakova, et. al., "Electromagnetic ELF radiation from earthquake regions as observed by low-altitude satellites", Geophysical Research Letters, Vol. 19, No. 2, pages 91-94, January 24, 1992.
3. M. Parrot, "Statistical study of ELF/VLF emissions recorded by a low-altitude satellite during seismic events", Journal of Geophysical Research, Vol. 99, No. A12, pages 23,339-23,347, December 1, 1994.
4. Dallas Semiconductor, MAX1873 Li+ Charge Controller Kit, July1 2001, http://www.maxim-ic.com/quick_view2.cfm/qv_pk/3105.
5. Power-One Series Single Output Power Regulator, June 2002, http://www.power-one.com/.
6. Wertz, J.R., and Larson, W.J., *Space Mission Analysis and Desig*n, 3rd Ed., Microcosm Press, El Segundo, CA, 1999.
7. Menges, B.M., Guadiamos, C.A., and Lewis, E.K., "Dynamic Modeling of Micro-Satellite Spartnik's Attitude", San Jose State University, http://www.engr.sjsu.edu/spartnik/adac.html.
8. White, J., "Microsat Motion, Stabilization, and Telemetry", AMSAT-NA, September 1990, http://coloradosatellite.com/Papers/Motion.html.
9. Kim, K., "Analysis of Hysteresis for Attitude Control of a Microsatellite", San Jose State University, http://www.engr.sjsu.edu/spartnik/adac.html.
10. Swartout, M., "Attitude Determination and Control, Sapphire Notes", http://students.cec.wustl.edu/~sapphire/design/log/sec8adc/8.1.html.